ELSEVIER

Journal of Power Sources 102 (2001) 302–309

JOURNAL OF POWER SOURCES

www.elsevier.com/locate/jpowsour

The effects of pulse charging on cycling characteristics of commercial lithium-ion batteries

Jun Li, Edward Murphy, Jack Winnick, Paul A. Kohl*

School of Chemical Engineering, Georgia Institute of Technology, Atlanta, GA 30332-0100, USA

Received 16 April 2001; accepted 15 May 2001

Abstract

The effects of a pulse charging technique on charge–discharge behavior and cycling characteristics of commercial lithium-ion batteries were investigated by comparison with the conventional direct current (dc) charging. The impedance spectra and cycling voltammograms of Li-ion batteries cycled by both protocols have been measured. The individual electrodes in the batteries have also been examined using XRD and SEM. The results show that pulse charging is helpful in eliminating concentration polarization, increasing the power transfer rate, and lowering charge time by removing the need for constant voltage charging in the conventional protocol. Pulse charging interrupts dc charging with short relaxation periods and short discharge pulses during charging, and also improves the active material utilization giving the battery higher discharge capacity and longer cycle life. Impedance measurements show that the magnitude of the interfacial resistance of the batteries cycled both by pulse charging and dc charging is small. However, at the same number of cycles, the interfacial resistance of the pulse charged battery is larger than that of dc charged. The batteries after 300 cycles charged by pulse charging show higher peak currents during both forward and reverse scans indicating higher reversibility of the electrodes. XRD and SEM studies of the individual electrodes indicate that pulse charging maintains the stability of the $LiCoO_2$ cathode better than dc charging and inhibits the increase in the thickness of the passive film on the anode during cycling.

Keywords: Lithium-ion batteries; Pulse charging technique; Capacity fade

1. Introduction

Commercial lithium-ion batteries are playing an important role as supplies for cellular phones, portable computers, camcorders, and other electronics. They often employ layered $LiCoO_2$ as the cathode material and graphitized carbon as the anode material. This configuration elicits high working voltage and energy density. During the charging process, the lithium ions are deintercalated from the cathode and intercalated into the anode through a nonaqueous electrolyte. Correspondingly, the cathode potential increases, Co(IV) cations are formed, and the anode potential decreases to nearly 0 V with respect to lithium metal. The cathode material in the state of $Li_{0.5}CoO_2$ retains the same layered structure as $LiCoO_2$ [1], and will become unstable when further oxidized. In addition, the nonaqueous electrolytes become easier to decompose due to thermodynamic instability and the metallic lithium is deposited on the anode at the higher battery charging voltage. An upper voltage limit during charging is essential for commercial lithium-ion battery chargers.

The conventional lithium-ion battery charging occurs in two steps, the battery is charged at a constant current (e.g. 1/3 C) until the potential reaches the upper voltage limit (4.1 or 4.2 V) followed by constant voltage charging until the current reaches a predetermined small value. The constant voltage charging seriously extends the charging time. It is well-known that lithium ion diffusion in the electrode is the rate-determining step in the charging process. The slow lithium ion diffusion inevitably results in concentration polarization, especially at the high current charging, bringing the battery voltage rapidly to the upper voltage limit. Alternatively, the constant voltage charging drops the current to the pre-set limit before the active material in the electrode is completely utilized.

In order to overcome these problems, the pulse-charging can be used for lithium-ion batteries, where short relaxation periods and short discharge pulses are applied during the charging process. The short relaxation periods and discharge pulses interspersed during the charging process can effectively eliminate the concentration polarization

* Corresponding author. Tel.: +1-404-894-2893; fax: +1-404-894-2866.
E-mail address: paul.kohl@che.gatech.edu (P.A. Kohl).

0378-7753/01/$ – see front matter
PII: S0378-7753(01)00820-5

and increase the power transfer rate, thus improving the active material utilization and accelerating the charging process [2].

In this paper, the cycling characteristics and electrochemical behavior of lithium-ion batteries charged by the pulse charging were compared with that a traditional constant current–constant voltage (dc) charging using impedance spectroscopy and cyclic voltammogram. On the basis of previous research [3], the microstructure of the electrodes in the batteries after cycling under two kinds of charging protocols were also studied using scanning electron microscopy (SEM) and X-ray diffraction (XRD).

2. Experimental

The commercial lithium-ion batteries used in this study were Sony US18650S cells with nominal capacity of 900 mAh. The batteries charged by pulse charging, developed by enrev Corporation [4], were cycled under the following scheme: the battery was charged at 1 or 0.5 C average to 4.2 V, kept for 0.5 h at open-circuit, and then discharged at the 1 C rate down to 3.0 V. The batteries charged by dc charging were cycled according to the following scheme: the battery was charged at a constant current of 1 C to 4.2 V, the battery voltage was held constant at 4.2 V until the current dropped to 25 μA, the battery was kept for 0.5 h at the open-circuit, and then discharged at the 1 C rate down to 3.0 V. The batteries charged by both protocols were kept for 0.5 h at open-circuit between two consecutive cycles. At the fully discharged state, the open circuit voltages of the batteries charged by both protocols were between 3.6 and 3.7 V. Impedance measurements of the lithium-ion batteries were carried out by a potentiostat (EG & G PARC Model 273A), equipped with a lock-in amplifier (EG & G PARC Model 521C) and controlled by impedance software Model 398. The amplitude of the alternating current signal was 5 mV over the frequency range between 50 kHz and 25 MHz. Cyclic voltammograms (CV) of the batteries were measured between cut-off voltages of 3.0 and 4.2 V with scan rate of 0.05 mV. Both electrochemical studies were conducted on the batteries when in the fully discharged state after being kept at open circuit for 1 h. The cathodes were used as working electrode and the anode as both the counter and reference electrodes.

Following the cycling experiment, the discharged batteries were carefully disassembled in a dry box. The cathodes and anodes were immediately placed into a diethyl carbonate solution (DEC, ≥99+%, Aldrich) for 5 h to remove the lithium salts adsorbed on the electrodes. The treated electrodes were dried in the dry box and prepared for microscopy examination. The structural changes of the electrode materials were investigated with XRD (Cu Kα radiation and graphite filter at 45 kV and 40 mA), and the surface morphologies were observed by means of a scanning electron microscopy (SEM, Hitachi S-800).

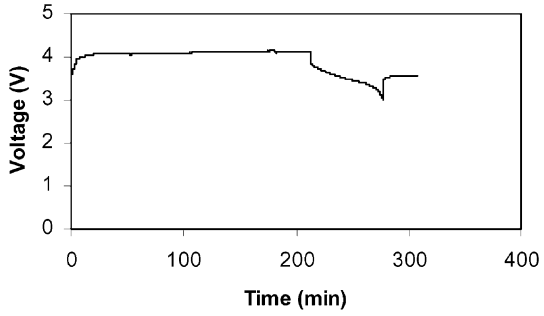

(a)

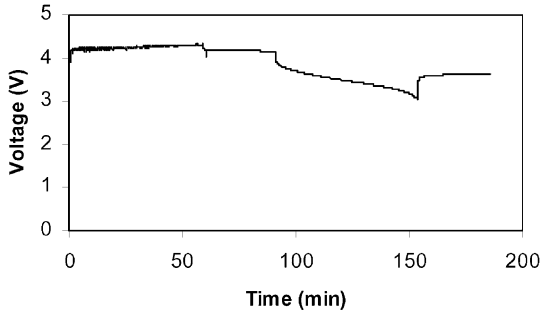

(b)

Fig. 1. The 1 C charge–discharge rate curves of the batteries during 1 cycle using two different charging protocols: (a) dc charging protocol; (b) pulse charging protocol.

3. Results and discussion

3.1. Charging characteristics of two charging protocols

Fig. 1 shows the charge–discharge curves of the batteries charged by the two protocols. At the 1 C charging rate, approximately 1 h was needed to fully charge the battery by the pulse charging method, while dc charging process required about 3.5 h. Because the pulse charging protocol eliminates concentration polarization by utilizing short relaxation periods and short discharge pulses, the electrode potentials should be at a quasi-equilibrium state at every point during charging, the batteries are already fully charged when reaching the limiting voltage. Thus, the pulse charging increases the power transfer rate and reduces the charging time of the lithium-ion batteries by removing the constant-voltage charging.

3.2. Cycling characteristics of two charging protocols

The discharge capacities of the lithium-ion batteries charged by the two charging protocols as a function of the number of cycles are shown in Fig. 2. All of the initial discharge capacities of the lithium-ion batteries are higher than the nominal capacity of the batteries (900 mAh). Compared with the discharge capacity of the battery charged by dc charging process at the 1 C charge–discharge rate, the

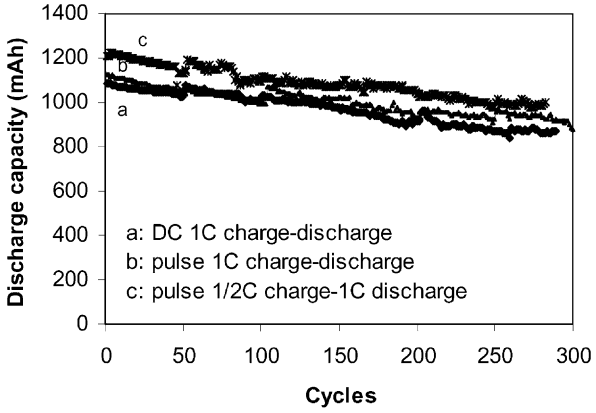

Fig. 2. Cycling performance of lithium-ion batteries using different protocols: (a) dc charging 1 C charge–discharge rate; (b) pulse charging 1 C charge–discharge rate; (c) pulse charging 0.5 C charge and 1 C discharge.

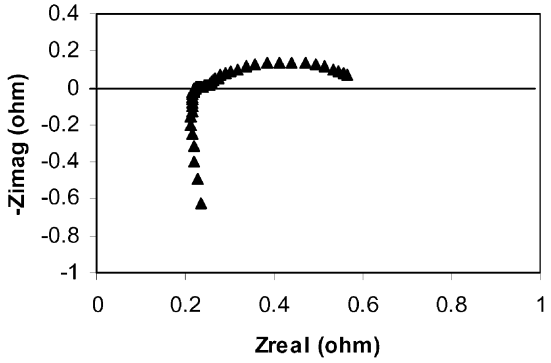

Fig. 3. Impedance spectrum of the commercial lithium-ion battery at fully discharged state after 250 cycles by pulse charging protocol at 1 C charge–discharge rate.

battery charged by pulse charging shows higher discharge capacity at the same charge–discharge rate. Further, the battery charged by pulse charging process at the 0.5 C charge rate followed by 1 C rate discharge has the highest discharge capacity. Although exhibiting a higher capacity fade-rate during the initial cycles, the capacity fade rate of the batteries charged by pulse charging is more stable than that dc charging. The full cycling tests that 1600 cycles will be completed before the discharge capacity of the battery charged by pulse charging decreased to 700 mAh, only about 700 cycles brought the dc charged batteries to this same capacity. Since both of the charging protocols have the same upper voltage limits and the proved similar charge–discharge efficiencies (nearly 100%) at the same charge–discharge rate, the higher discharge capacity of the battery charged by pulse charging indicates the pulse protocol can fully utilize the active materials in the battery without over-charging and sacrificing cycling life.

3.3. Electrochemical characteristics

3.3.1. Electrochemical impedance spectrum

The Nyquist plot of a commercial lithium-ion battery is mainly comprised of an inductive tail at high frequency followed by two semicircles of different size at the medium and low frequencies [3,5,6], as shown in Fig. 3. The inductance behavior of the lithium-ion battery is attributed to the porous structure of the electrodes. No contributions to the variation in the electrical and electrochemical characteristics of the battery during cycling are seen, nor is there any influence on the other parameters obtained from the impedance spectrum [6–8]. Thus, the inductive tail in Nyquist plot can be excluded when analyzing the changes in impedance spectrum of the lithium-ion battery during cycling.

Fig. 4 compares the Nyquist plots of the fully discharged lithium-ion battery as a function of cycle number, cycled by pulse charging process at 0.5 C rate charging and 1 C rate discharging. The size of the semicircle at low frequency continuously increases with the number of cycles, while the size of the semicircle at medium frequency is very small (<0.05 Ω), remains constant during cycling. In addition, there is a very small linear spike following the low frequency semicircle in the impedance spectrum of the fresh battery, associated with the diffusion of the lithium ions in the electrolyte, into and from the electrode. This small diffusion impedance rapidly disappears with increasing cycles due to the relative increase of electrochemical reaction resistance.

Hence, only the parameters related to the semicircle at low frequency change during cycling are useful for prediction of the cycle life of the battery. Under these conditions, a simplified equivalent circuit represented in Fig. 5a is employed to determine the cycle life related to the impedance parameters. The corresponding complex plane diagram containing a semicircle is shown in Fig. 5b [9], in which R_Ω is the value of the high-frequency intercept of the semicircle on the real part of impedance modulus and R_{ct} is the diameter of the semicircle. Note here that R_Ω is approximately equal to the ohmic resistance of the battery including the resistance of the electrolyte, current collectors, battery terminals and internal connectors in the battery [6]. The charge-transfer resistance R_{ct} results from the both the cathode and anode and can be defined as the interfacial

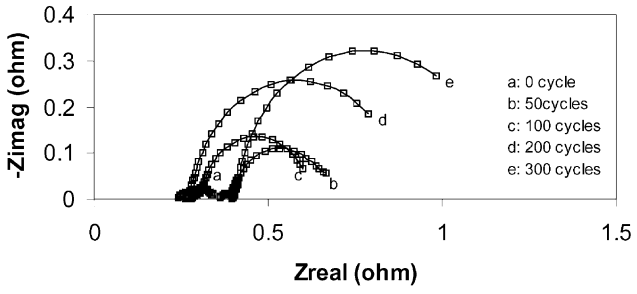

Fig. 4. Impedance spectra of fully discharged lithium-ion batteries with different cycle number by pulse charging at 0.5 C charge–1 C discharge rate.

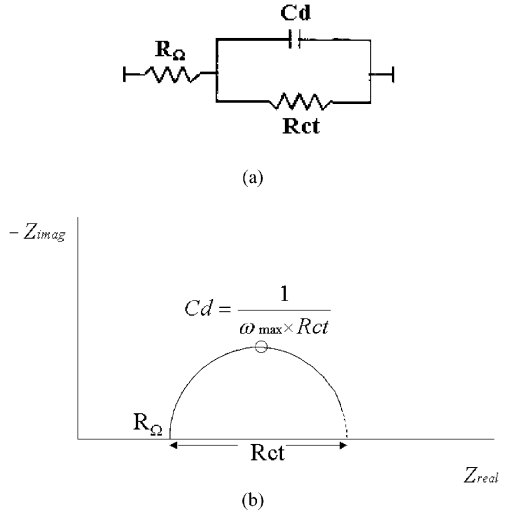

Fig. 5. Simplified equivalent circuit of a lithium-ion battery (a) and corresponding complex plane impedance spectrum (b).

resistance, distinguished from the charge transfer resistance in the single electrode.

The magnitudes of the parameters obtained from the impedance spectra of the batteries cycled by both pulse charging and dc charging protocols are shown in Fig. 6.

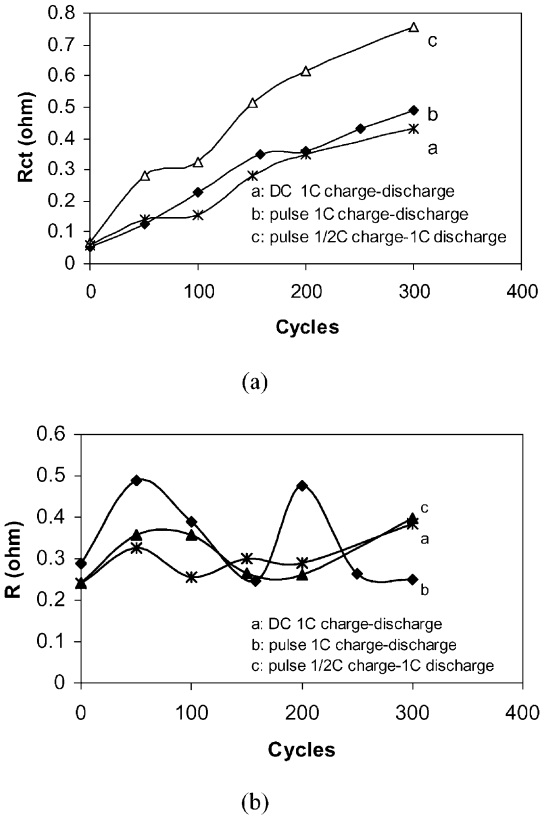

Fig. 6. Impedance parameters as a function of cycle number of lithium-ion batteries cycled by both pulse and dc charging protocols: (a) interfacial resistance; (b) ohmic resistance.

It can be seen that R_Ω of the batteries cycled by both pulse and dc charging processes fluctuate around a constant value with increase in cycle number. This indicates that the ohmic resistance of the battery is stable during cycle and independent of the charging protocol or charge–discharge regimen. On the other hand, the magnitudes of R_{ct} of the batteries increase continuously on cycling, consistent with the discharge capacity fade of the batteries.

The R_{ct} of the batteries with the same cycle number by both pulse and dc charging at the same charge–discharge rate have similar values. However, the magnitude of R_{ct} of the battery cycled by pulse charging at the 0.5 C charge–1 C discharge rate are higher than that of the batteries cycled by both pulse and dc charging processes at the 1 C charge–discharge rates. This behavior is the reverse of the discharge capacity of the batteries.

The cycling life of the lithium ion battery depends on the stability of the electrode materials and the interfaces among the anode, cathode and electrolyte. Since the interfacial resistance obtained from the impedance spectrum are mainly related to the surface film and interfacial charge-transfer resistance of both the cathode and anode [10], it could be concluded that the increase in the interfacial resistance of the battery can not reflect directly the discharge capacity fade, while it could be used to predict the cycle life. In fact, all the R_{ct} of the batteries are very low even after 300 cycles. The increase in the interfacial resistance of the battery indicates an increase in the surface film resistance and interfacial charge-transfer resistance, both of which may result from the interfacial reaction between the electrode and the electrolyte. The battery cycled by pulse charging at the slower charging rate has a higher discharge capacity indicating that more Li^+ ions are extracted from the cathode active materials. The higher portion of Co(IV) cations are thus formed in the cathode when the battery is at the fully charged state and the cathode will have stronger oxidizing power [11]. Therefore, the cathode is more likely to react with the electrolyte and form a layer film on the cathode, contributing to a higher interfacial resistance of the battery.

3.3.2. Cyclic voltammograms

Fig. 7 presents a comparison of cyclic voltammograms of the lithium-ion batteries after 300 cycles by dc charging protocol at 1 C charge–discharge rate, and pulse charging protocol at 0.5 C charge–1 C discharge rates. The forward scan is associated with the charge process, in which the Li^+ ions are extracted from the cathode and inserted into the anode, the reverse scan is associated with the discharge process of the battery, in which the Li^+ ions are removed from the anode and reinserted into cathode. It can been seen that peaks appear in both the charge and discharge processes, peak currents for the pulse charged battery are larger than that by dc charging protocol during both

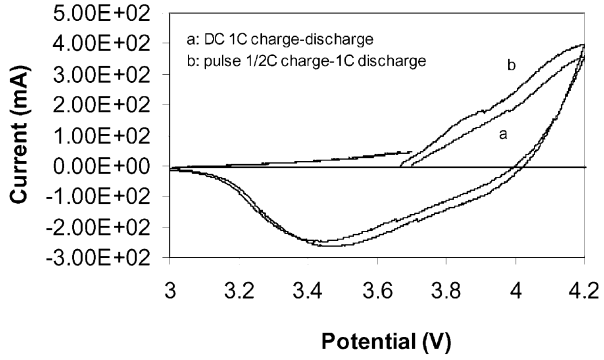

Fig. 7. CV of batteries after 300 cycles by different charging protocols. Scan rate is 0.05 mV/s with scan cut-off voltage of 3.0 and 4.2 V: (a) dc charging at 1 C charge–discharge rate; (b) pulse charging at 0.5 C charge–1 C discharge.

forward and reverse scans. The magnitude of the peak currents reflects the rate of the Li^+ ions extraction and insertion; they indicate the extent of the deterioration of the electrode materials and interface between the electrode and the electrolyte. After 300 cycles, the pulse charged battery that has a higher forward and reverse scan peak current (in the CV) is that with the higher discharge capacity, yet it is the battery with higher interfacial resistance. Thus, the interfacial resistance seen in impedance spectrum is not the only factor causing the battery capacity fading.

3.4. Electrode microstructure

The cycled batteries were taken apart in a dry box and microstructures of the individual electrodes examined using SEM and XRD. For comparison, a fresh battery was also disassembled. The surface morphologies of the cathodes are shown in Fig. 8. It can be seen that the active material on the current collector stays compact after 300 cycles, but cracks are observed on some active material particles in all cathodes (cycled by both pulse and dc charging protocols) in comparison with the cathode surface in the fresh battery. From the appearance, it can be concluded that these cracks

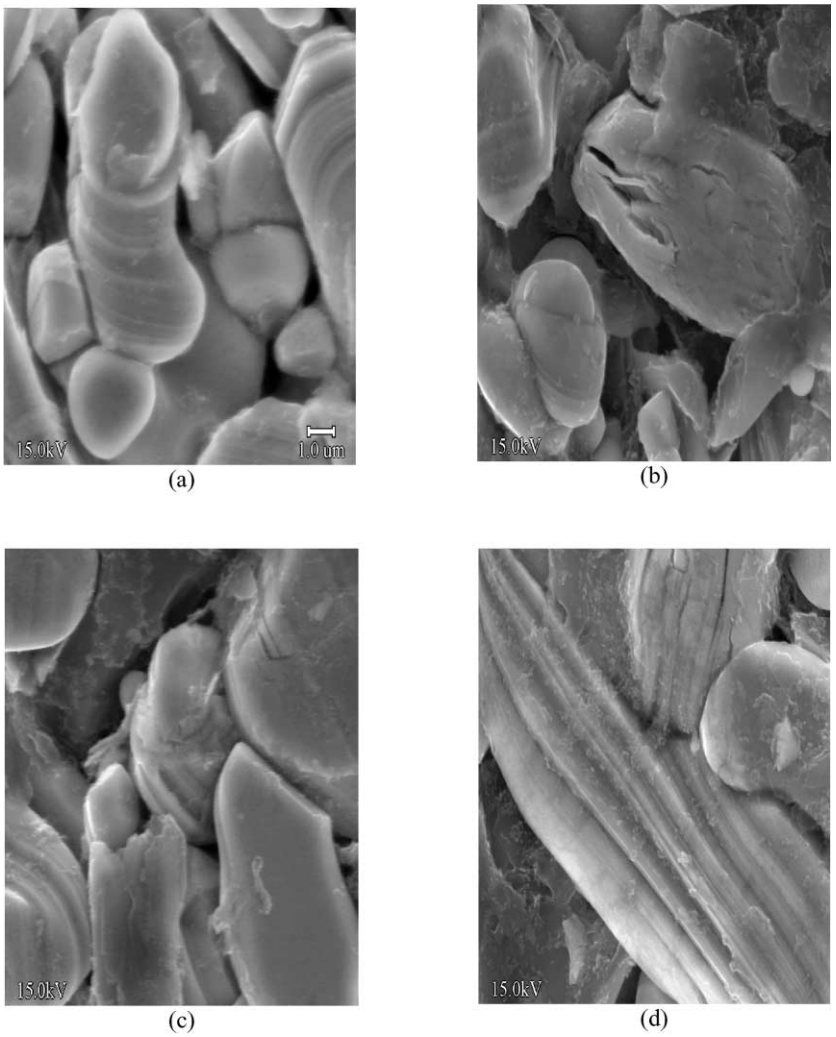

Fig. 8. Micrographs of cathodes in the fully discharged fresh and 300 cycled lithium-ion batteries by different protocols: (a) fresh cathode; (b) dc charging 1 C charge–discharge rate; (c) pulse charging 1 C charge–discharge rate; (d) pulse charging 0.5 C charge–1 C discharge.

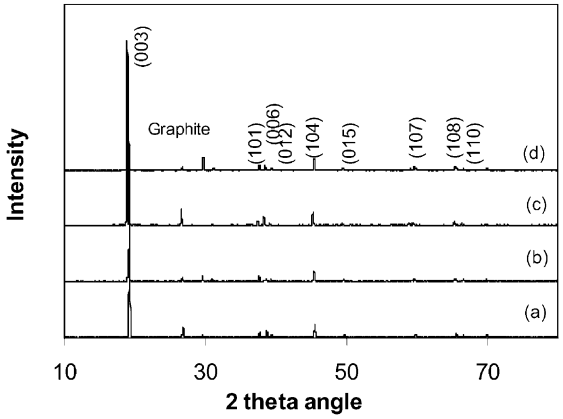

Fig. 9. XRD patterns for cathode materials in the fully discharged fresh and 300 cycled lithium-ion batteries by different protocols: (a) fresh cathode; (b) dc charging 1 C charge–discharge rate; (c) pulse charging 1 C charge–discharge rate; (d) pulse charging 0.5 C charge–1 C discharge.

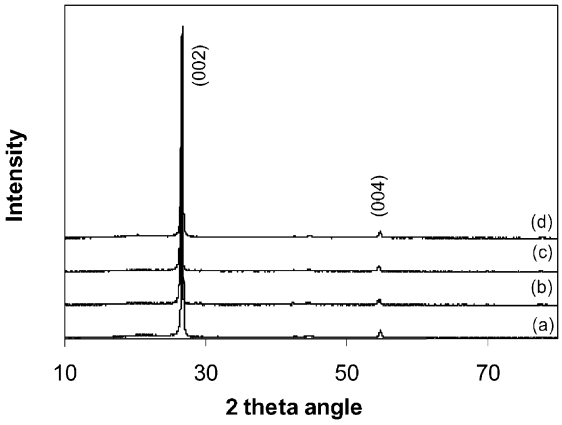

Fig. 10. XRD patterns for anode materials in the fully discharged fresh and 300 cycled lithium-ion batteries by different protocols: (a) fresh cathode; (b) dc charging 1 C charge–discharge rate; (c) pulse charging 1 C charge–discharge rate; (d) pulse charging 0.5 C charge–1 C discharge.

in the active materials particles do not result from the mechanical force during electrode production, but from the stress during cycling. The cathode active material employed in the Sony batteries is layered $LiCoO_2$. During cycling delithiation/lithiation processes in the cathode inevitably cause a volume change in the $LiCoO_2$ particles and produce a stress, inducing the internal cracks. XRD patterns of the corresponding cathode materials are shown in Fig. 9. During cycling, the appeared characteristic peaks of the $LiCoO_2$ remain the same, indicating no a new phase is produced. However, the relative peak intensity ratios between the (0 0 3) and (1 0 1) or (1 0 4) planes are different, indicating a change in the structure of the $LiCoO_2$ phase. The relative intensity of the main peak (0 0 3) of cathode material after 300 cycles by pulse charging process at 1 C charge–discharge rate is close to that of the fresh battery, higher that of the other two cycled batteries. The main peak (0 0 3) of the cathode material cycled by dc charging process at 1 C charge–discharge rate has the lowest relative intensity.

In the $LiCoO_2$ phase, alternate layers of Li and Co cations occupy the octahedral sites of a compact cubic close packing of oxide anions. The (0 0 3) peak intensity decrease occurs when a cobalt atom occupies some of the octahedral sites of the lithium layer [12,13]. Hence, a decrease in the relative intensity of the (0 0 3) peak during cycling indicates that the cation in the well-layered $LiCoO_2$ becomes disordered and a portion of the lithium ions in the cathode becomes inactive. In addition to the cracks in the $LiCoO_2$ particles, the cation disorder in $LiCoO_2$ have been clearly confirmed using electron diffraction and TEM [14]. This is also believed to come from the strain induced by the intercalation–deintercalation of lithium ions during cycling. Both contribute to the capacity fade of the cathode. The cathode material cycled by the pulse charging protocol, which has the higher relative intensity of (3 0 0) peak, indicates that this protocol better maintains the structure of cathode material due to short relaxation periods and short discharge pulses during charging. This lowers the polarization, and thus allows the Li^+ ions to be more uniformly extracted from or reinserted into the cathode materials.

XRD patterns of the anode materials in the fresh battery and cycled batteries by both dc and pulse charging protocols are shown in Fig. 10. It is clear that the anode material is graphitized carbon because of the strong (0 0 2) peak. None of the intensities or positions of the characteristic peaks of the carbon electrodes change during cycling. The small amorphous peak at about $2\theta = 20^\circ$ in the electrode is also unchanged, which indicates the stable graphitization of the carbon anode during cycling. The surface morphologies of the corresponding anode active material are shown in Fig. 11. Compared with the fresh anode surface, the passive films on the surface of the anodes increase in the thickness during cycling by both dc and pulse charging protocols. The anode cycled by dc charging protocol at 1 C charge–discharge rate has the thickest passive film on the surface, we can not even identify the true surface morphology of the carbon. In comparison, the anode cycled by pulse charging has a thinner passive film on the surface, especially after the lower charging rate. The passive film on the anode can function as a shield that effectively hinders the Li^+ ions from penetrating through to the active anode [15], thus contributing to increases in the surface resistance. On the other hand, the process of passive film increase itself must also cause capacity fade because of the consumption of the electrolyte components. It is not clear how the increase of the passive film on the carbon electrode influences the capacity drop, despite the many investigations of the irreversible capacity loss in the carbon anode due to the formation of a solid-electrolytic interface in the initial charge–discharge cycle [16,17].

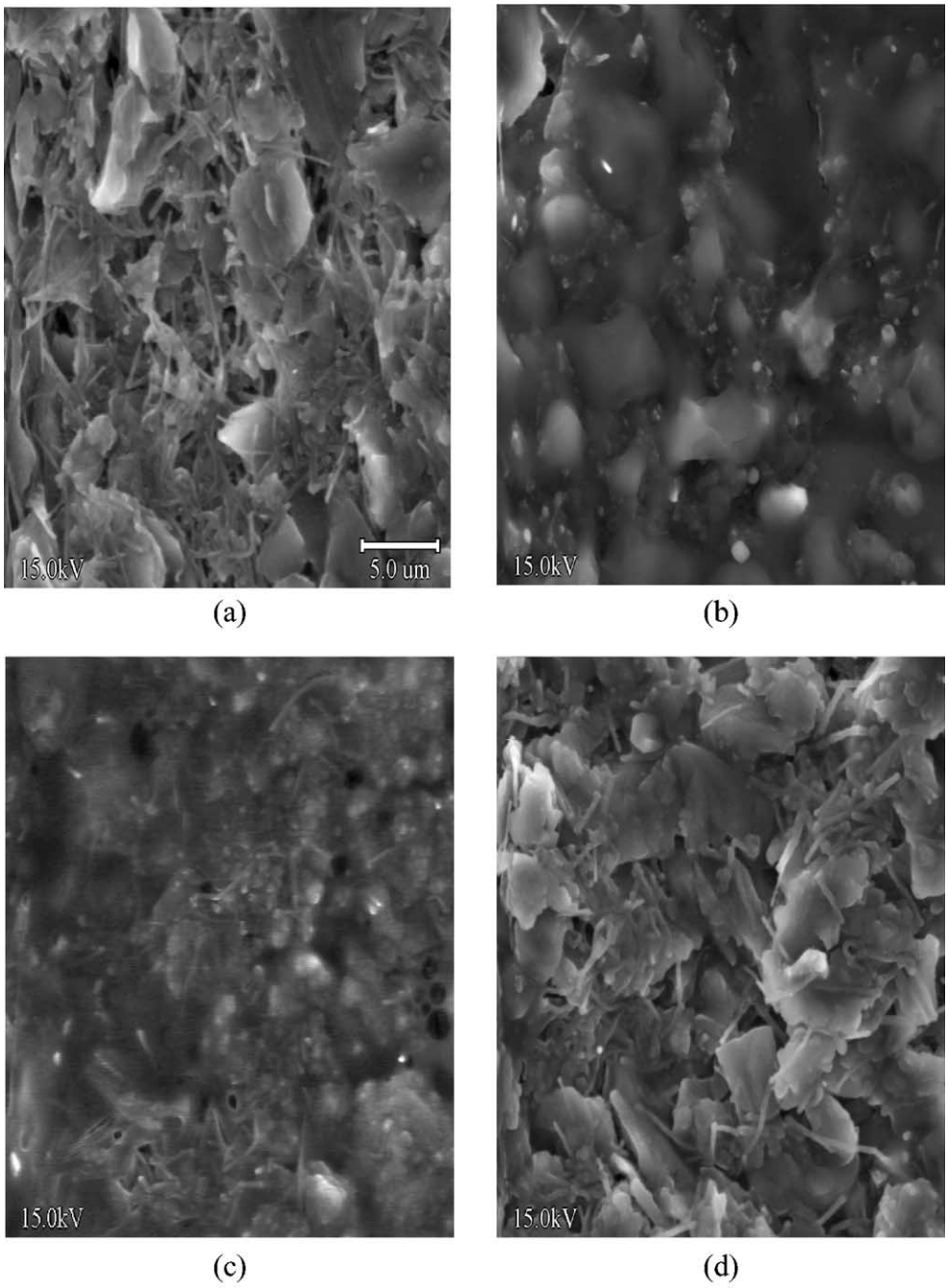

Fig. 11. Micrographs of anodes in the fully discharged fresh and 300 cycled lithium-ion batteries by different protocols: (a) fresh anode; (b) dc charging1 C charge–discharge rate; (c) pulse charging 1 C charge–discharge rate; (d) pulse charging 0.5 C charge–1 C discharge.

4. Conclusion

A new charging protocol for the lithium-ion battery, involving a short relaxation periods and short discharge pulses during charging appears helpful in eliminating concentration polarization and increasing the power transfer rate. This lowers the charging time and improves the active material utilization, yielding higher discharge capacity and longer cycle life.

Impedance analysis shows that the magnitudes of the interfacial resistances of the batteries cycled both by pulse charging and conventional dc charging protocols are small. However, at the same cycle number, the interfacial resistance of the battery cycled by pulse charging is larger than that by conventional protocol. Studies of XRD and SEM on the individual electrode indicate that the pulse charging protocol maintains the structure stability of the cathode active material $LiCoO_2$ better

and inhibits increase in the thickness of the passive film on the carbon anode.

Acknowledgements

The enrev Corporation provided partial funding for this work.

References

[1] V. Ganesh Kumar, N. Munichandraiah, A.K. Shukla, J. Appl. Electrochem. 27 (1997) 43–49.
[2] B. Tsenter, Y. Podrazhansky, Charging algorithm for rapid battery charge, in: Proceedings of the Meeting Abstracts of 188th Electrochemical Society Meeting, Chicago, IL, 8–13 October 1995.
[3] Jun Li, Edward Murphy, Jack Winnick, Paul A. Kohl, J. Power Source, submitted for publication.
[4] Podrazhansky et al., US Patent No. 5,504,415 (1996).
[5] G. Nagasubramanian, J. Power Sources 87 (2000) 226–229.
[6] S. Rodrigues, N. Munichandraiah, A.K. Shukla, J. Solid State Electrochem. 3 (1999) 397–405.
[7] F.C. Laman, M.W. Matsen, J.A.R. Stiles, J. Electrochem. Soc. 133 (1986) 2441.
[8] N.A. Hampson, S.A.G.R. Karunathilaka, R. Leek, J. Appl. Electrochem. 10 (1980) 3.
[9] F. Huet, J. Power Sources 70 (1998) 59–69.
[10] C. Wang, A. John Appleby, E. Little, J. Electroanal. Chem. 497 (1998) 33–46.
[11] D. Zhang, B.S. haran, A. Durairajan, R.E. White, Y. Podrazhansky, B.N. Popove, J. Power Sources 91 (2000) 122–129.
[12] M. Yoshio, H. Tanaka, K. Tominaga, H. Noguchi, J. Power Sources 40 (1992) 347–353.
[13] E.-D. Jeong, M.-S. Won, Y.-B. Shim, J. Power Sources 70 (1998) 70–77.
[14] H. Wang, Y.-I. Jang, B. Huang, D.R. Sadoway, Y.-M. Chiang, J. Electrochem. Soc. 146 (1999) 473.
[15] A.M. Andersson, K. Edstrom, N. Rao, A. Wendsjo, J. Power Sources 81/82 (1999) 286–290.
[16] D. Aurbach, B. Markovsky, I. Weissman, E. levi, Y. Ein-Eli, Electrochim. Acta 45 (1999) 67–86.
[17] Y. Matsumura, S. Wang, J. Mondori, J. Electrochem. Soc. 142 (1995) 2914.